Available online at www.sciencedirect.com
ScienceDirect
Earth and Planetary Science Letters 261 (2007) 620–634
EPSL
www.elsevier.com/locate/epsl

Depth of formation of subcontinental off-craton peridotites

Dmitri A. Ionov [a,b,*], Albrecht W. Hofmann [a]

[a] Max-Planck-Institut für Chemie, Postfach 3060, D-55020 Mainz, Germany
[b] LTL, UMR-CNRS 6524, Département de Géologie, Université J. Monnet, 23 rue P. Michelon, 42023 Saint-Etienne, France

Received 16 January 2007; received in revised form 16 July 2007; accepted 17 July 2007
Available online 25 July 2007
Editor: R.W. Carlson

Abstract

The subcontinental lithosphere is thought to be a mantle region from which melts have been extracted. This process lowers Ca and Al contents, thus making the lithosphere more refractory, but little is known about the depth at which those melts are extracted. Experimental evidence suggests that iron might be used as a pressure gauge. At high pressures, melting depletes the residue in iron, but at lower pressures ($P<2$ GPa) and low degrees of melting, the residue must be enriched in iron. However, such Fe-enrichments have never been documented in mantle peridotites. Here we show that Fe–Al relationships in mantle xenoliths from central Asia match those predicted by melting experiments both at low and moderate pressures. We find that Fe is negatively correlated with Al in fertile (>3.5% Al_2O_3) peridotites consistent with 0–6% melting at 1 GPa. In contrast, Fe is positively correlated with Al in more refractory peridotites produced by higher degrees (up to 35%) of partial melting at 2–4 GPa. The current position of these rocks in the lithosphere estimated from thermo-barometry may be quite different from the depth of melt extraction. We attribute this to tectonic processes during the transformation of an initial assemblage of melting residues into mature continental lithosphere.
© 2007 Elsevier B.V. All rights reserved.

Keywords: continental lithospheric mantle; residual peridotite; partial melting; melting depth; lithosphere formation

1. Introduction

One of the rarely contested paradigms of igneous petrology is that the subcontinental lithosphere is made up of residues after different degrees of melt extraction from originally more "fertile" mantle rocks (Frey and Green, 1974; Nickel and Green, 1984; McDonough, 1990; Menzies, 1990). Experimental work has firmly established that the melting residues are invariably depleted in the so-called "basaltic components": CaO, Al_2O_3, Na_2O as the melting progresses. By contrast, the behaviour of iron during partial melting is pressure-dependent and hence can be used to infer the depth of melt extraction (Walter, 2003; Herzberg, 2004 and references therein). Melting residues at high pressures are strongly depleted in iron and have high Mg-numbers [$Mg/(Mg+Fe)_{at}$] whereas at low pressures (<2 GPa) the iron content in the residues increases at low melting degrees (Fig. 1a). In particular, the continental lithospheric mantle (CLM) beneath the Archean–Paleoproterozoic domains (cratons) typically has low FeO and high Mg-numbers and is thought to have been formed by high degrees of melting at ≥4–5 GPa (Fig. 1b) (Hanson and Langmuir, 1978; Jordan, 1979; Boyd, 1989).

Although the younger, off-craton CLM is believed to be produced by shallow partial melting, the exact conditions and geodynamic settings of the melting

* Corresponding author. LTL, UMR-CNRS 6524, Département de Géologie, Université J. Monnet, 23 rue P. Michelon, 42023 Saint-Etienne, France. Tel.: +33 47748 1512; fax: +33 47748 5108.
E-mail address: dmitri.ionov@univ-st-etienne.fr (D.A. Ionov).

0012-821X/$ - see front matter © 2007 Elsevier B.V. All rights reserved.
doi:10.1016/j.epsl.2007.07.036

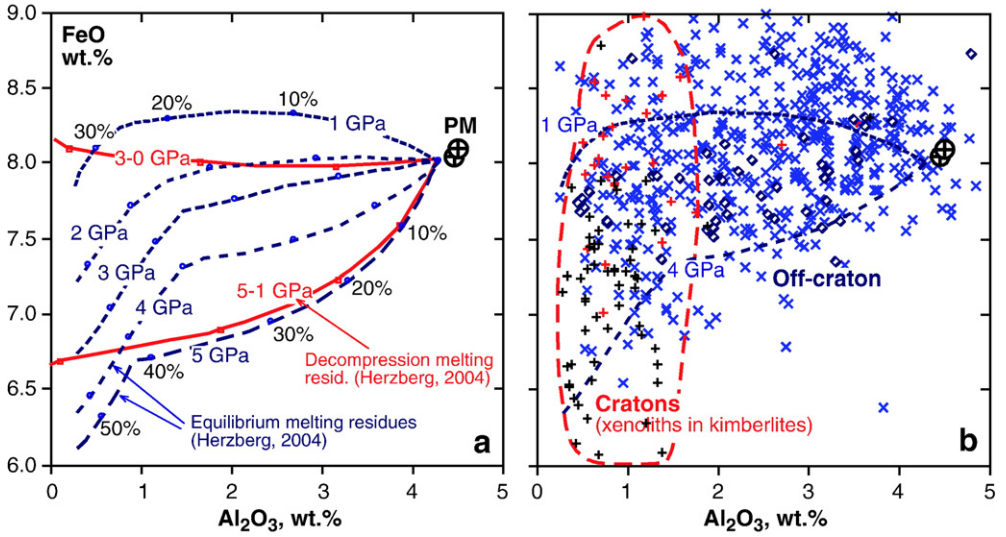

Fig. 1. Plots of FeO vs. Al_2O_3 in melting residues and mantle peridotites. (a) Experimental melt extraction residues formed by equilibrium (fixed pressure) partial melting (dashed lines; melting degrees are indicated) and polybaric decompression fractional melting (continuous lines) of a fertile natural peridotite (Herzberg, 2004). FeO in the residues of shallow melting (1 GPa) increases from 0 to ~10% of melting; FeO degreases during melting at greater depths. Large circles with crosses are primitive mantle models (McDonough and Sun, 1995; Palme and O'Neill, 2003). (b) Off-craton peridotite xenoliths from worldwide localities (diagonal crosses) after (Canil, 2004), cratonic xenoliths (black crosses, low-T; grey or red crosses, high-T) (Boyd et al., 1997; Lee and Rudnick, 1999; Kopylova and Russell, 2000) and peridotites from the Horoman massif (rhombs) (Takazawa et al., 2000); some 70 Fe-rich wehrlites (Ca/Al=~2–7) from the data base of (Canil, 2004) have not been plotted. Xenoliths with FeO>9% (i.e. off-scale on the diagram) have been also reported. The broad scatter of data points is mainly due to melting at different depths and post-melting Fe-enrichments.

processes are not well understood. A major difficulty is that the initial melting residues are commonly affected by "metasomatic" interaction with late-stage, commonly Fe-rich, melts as well as by alteration processes during and after the transport of the mantle rocks to the surface for abyssal, massif and ophiolite peridotites as well as mantle xenoliths in volcanic rocks (Frey and Green, 1974; Menzies et al., 1987; Kelemen et al., 1992; Boyd et al., 1997; Saal et al., 2001; Bodinier and Godard, 2003; Ionov et al., 2005a). Moreover, melting residues produced at different depths as well as rocks affected by late-stage processes may be juxtaposed in tectonically active areas (e.g. Kelemen et al., 1998). This obscures the chemographic melting relationships in exposed mantle rocks and causes the co-variation plots of major oxides vs. Fe in those rocks to be dominated by Fe scatter (e.g. Al–Fe; Fig. 1b).

In this paper, we provide high-quality major element analyses for a series of fresh mantle peridotites that have remained relatively unaffected by melt metasomatism. Fe–Al and other major element co-variations in those samples, together with recently published data on a similar suite (Ionov et al., 2005b), are used to assess their depth of origin. We demonstrate for the first time that the iron content in off-craton mantle xenoliths preserves the depth record of melt extraction, in line with results expected from experimental petrology. We also show that this depth of melt extraction can be very different from the depth where these rocks resided prior to their ejection through volcanic eruptions.

2. Samples, analytical techniques and data quality

2.1. Sample description

The samples in this study are fragments of CLM brought up to the surface by late Cenozoic basaltic magmas in central Asia: Mongolia (Tariat (Press et al., 1986)) and Baikal region (Vitim (Ionov et al., 1993)). These xenoliths are spinel and garnet peridotites with a broad range of compositions (and hence extents of melt extraction) including abundant fertile rocks. They contain little or no metasomatic minerals and largely retain chemical signatures of ancient partial melting (Press et al., 1986; Stosch et al., 1986; Ionov et al., 2005b).

The main part of our data set are new whole-rock major element analyses for over 40 xenoliths from the 0.5 Ma-old Shavaryn–Tsaram eruption centre (48°12′N, 100°E) in the Tariat region of central Mongolia (Table 1). Xenoliths from that locality were studied by Press et al. (1986), Ionov (1986) and Spettel et al. (1991). We analysed the majority of samples from those earlier

Table 1
XRF analyses of whole-rock Tariat xenoliths and reference samples (wt. %)

Sample	Rock	SiO_2	TiO_2	Al_2O_3	Cr_2O_3	ΣFeO	MnO	NiO	MgO	CaO	Na_2O	K_2O	P_2O_5	Total	CMI	Mg#	Ca/Al
MHP-1	Sp lh	45.50	0.16	3.92	0.37	8.21	0.13	0.26	38.08	3.12	0.29	0.01	0.01	100.1	0.22	0.892	1.07
79-1	Sp lh	45.06	0.15	4.13	0.41	8.20	0.13	0.26	38.70	2.94	0.27	0.01	0.01	100.3	0.35	0.894	0.96
79-2	Sp lh	45.46	0.16	4.23	0.42	7.99	0.13	0.25	37.66	3.17	0.31	0.03	0.02	99.8	0.27	0.894	1.01
79-3	Sp lh	44.60	0.10	3.06	0.36	7.88	0.13	0.28	41.60	2.28	0.20	bd	0.01	100.5	0.22	0.904	1.01
79-4	Sp lh	44.64	0.10	2.90	0.33	7.88	0.13	0.28	41.58	2.02	0.17	0.01	0.01	100.0	0.18	0.904	0.94
Mo-88	Sp hzb	44.76	0.03	1.06	0.39	7.95	0.12	0.31	44.51	0.64	0.08	0.07	0.02	99.9	0.54	0.909	0.81
Mo-89	Sp lh	43.89	0.02	1.70	0.37	8.07	0.13	0.30	43.90	1.20	0.13	0.05	0.03	99.8	0.57	0.907	0.96
Mo-90	Sp lh	44.63	0.06	2.13	0.42	7.72	0.12	0.29	42.83	1.76	0.14	0.02	0.03	100.2	0.27	0.908	1.12
Mo-91	Sp lh	44.56	0.05	2.61	0.42	7.69	0.13	0.28	41.46	2.35	0.27	0.01	0.02	99.8	0.25	0.906	1.21
Mo-92	Sp lh	44.45	0.07	2.14	0.41	7.50	0.12	0.30	43.42	1.65	0.15	0.04	0.01	100.3	0.31	0.912	1.04
Mo-93	Sp lh	43.97	0.08	2.14	0.39	7.49	0.12	0.30	43.36	1.67	0.18	0.07	0.02	99.8	0.35	0.912	1.06
Mo-94	Sp hzb	43.39	0.03	0.96	0.45	8.08	0.13	0.32	45.62	0.76	0.02	0.01	0.02	99.8	0.32	0.910	1.07
Mo-95	Sp lh	43.83	0.05	1.54	0.40	8.02	0.12	0.31	44.41	1.38	0.10	0.02	0.01	100.2	0.28	0.908	1.21
Mo-96	Sp lh	43.96	0.08	2.54	0.37	7.90	0.13	0.29	42.39	2.13	0.29	0.02	0.07	100.2	0.19	0.905	1.13
Mo-99-7	Sp lh	44.96	0.15	3.74	0.33	8.21	0.13	0.27	38.50	3.13	0.27	0.01	0.01	99.7	-0.66	0.893	1.13
Mo-101	Sp lh	45.40	0.19	4.33	0.41	8.04	0.13	0.25	37.17	4.10	0.38	0.01	0.01	100.4	0.22	0.892	1.28
Mo-102	Sp lh	45.15	0.07	2.59	0.42	7.61	0.12	0.28	41.42	2.37	0.16	0.02	0.03	100.2	0.26	0.907	1.23
Mo-103	Sp lh	44.48	0.05	2.23	0.50	7.74	0.12	0.29	42.44	1.79	0.08	0.02	0.01	99.7	0.19	0.908	1.08
Mo-104	Sp lh	45.11	0.11	2.85	0.36	7.95	0.13	0.27	40.95	2.23	0.20	0.02	0.05	100.2	0.23	0.902	1.05
Mo-105	Sp lh	46.60	0.21	5.07	0.45	7.57	0.13	0.23	35.41	4.17	0.43	0.01	0.01	100.3	0.10	0.893	1.11
MOG-1 [a]	Sp lh	45.91	0.18	4.47	0.40	8.09	0.14	0.23	36.54	3.63	0.42	bd	nd	100.0	nd	0.890	1.10
MOG-2 [a]	Sp lh	44.45	0.11	3.25	0.41	8.10	0.13	0.26	40.25	2.72	0.31	0.01	nd	100.0	nd	0.899	1.13
MOG-3	Sp lh	44.24	0.10	3.06	0.37	7.95	0.13	0.29	41.11	2.48	0.21	bd	0.02	100.0	0.40	0.902	1.10
MOG-4	Sp lh	44.98	0.11	3.29	0.41	7.83	0.13	0.27	40.21	2.87	0.24	bd	0.01	100.3	0.37	0.902	1.18
MOG-5	Sp lh	45.62	0.16	4.35	0.43	7.88	0.13	0.25	36.96	3.40	0.32	0.01	0.02	99.5	0.33	0.893	1.06
4230-16	Phl-sp lh	45.20	0.23	4.32	0.40	8.40	0.14	0.25	36.94	3.85	0.32	0.08	0.01	100.1	0.31	0.887	1.20
4399-23 [b]	Sp hzb	43.03	0.02	0.88	0.42	8.00	0.12	0.32	46.31	0.78	0.10	0.02	0.04	100.0	nd	0.912	1.20
4399-26 [b]	Sp hzb	43.39	0.05	1.29	0.34	8.48	0.13	0.32	45.41	0.62	0.11	0.04	0.02	100.2	nd	0.905	0.65
4500-8	Sp lh	45.37	0.18	3.84	0.35	8.34	0.14	0.26	38.02	3.22	0.33	0.01	0.02	100.1	0.35	0.890	1.13
4500-18 [b]	Sp hzb	43.97	0.03	0.72	0.26	7.28	0.11	0.32	46.56	0.52	0.11	0.07	0.04	100.0	nd	0.919	0.97
4500-19 [b]	Sp hzb	43.47	0.04	1.06	0.40	7.60	0.12	0.32	45.78	1.07	0.10	bd	nd	100.0	nd	0.915	1.36
4500-21	Sp lh	45.09	0.14	3.72	0.41	8.18	0.13	0.26	38.64	3.17	0.27	0.01	0.02	100.0	0.35	0.894	1.15
4500-26	Sp lh	45.29	0.16	3.82	0.37	8.16	0.13	0.26	38.26	3.24	0.31	0.01	0.03	100.0	0.23	0.893	1.14
4500-33	Sp lh	44.84	0.11	3.12	0.40	7.95	0.13	0.27	40.71	2.65	0.22	0.01	0.01	100.4	0.42	0.901	1.15
4594-4	Sp hzb	44.12	0.02	0.97	0.47	7.82	0.12	0.32	45.40	0.73	0.06	0.02	0.04	100.1	0.36	0.912	1.01
4594-6	Sp lh	45.14	0.16	3.98	0.38	8.08	0.14	0.25	38.20	3.24	0.30	0.01	0.03	99.9	0.37	0.894	1.10
53389	Gar-sp lh	45.42	0.18	4.70	0.31	7.97	0.14	0.23	36.86	3.82	0.36	0.00	0.01	100.0	0.35	0.892	1.10
8530-3 [b]	Sp lh	44.82	0.04	2.45	0.41	7.87	0.15	0.27	41.56	2.29	0.25	0.01	0.02	100.1	nd	0.904	1.26
8530-5a	Sp lh	44.66	0.05	2.28	0.49	7.78	0.13	0.28	41.16	2.29	0.43	0.03	0.08	99.7	nd	0.904	1.36
8530-18	Sp hzb	42.80	0.06	1.25	0.44	8.35	0.17	0.33	45.88	0.49	0.06	0.04	0.02	99.9	0.32	0.907	0.53
8530-24	Sp hzb	43.35	0.07	1.99	0.33	8.76	0.17	0.29	43.57	1.13	0.11	0.02	0.04	99.8	0.04	0.899	0.77
8531-40 [b]	Sp hzb	43.77	0.03	1.21	0.28	8.80	0.15	0.31	44.63	0.55	0.33	0.13	0.03	100.2	0.43	0.900	0.62
8531-42	Sp lh	44.12	0.05	2.19	0.75	7.38	0.13	0.28	42.29	2.44	0.15	0.02	0.05	99.9	nd	0.911	1.51
UBN (8)	Ref sa	45.36	0.11	3.35	0.39	8.42	0.14	0.29	40.09	1.38	0.13	0.03	0.01	99.73	-12.1	0.89	
RSD (8)		0.3%	1.6%	0.6%	0.4%	0.3%	1.1%	0.2%	0.5%	0.7%	10%	17%	13%	0.3%		0.03%	
JP-1 (5)	Ref sa	43.71	0.01	0.71	0.43	7.61	0.12	0.33	45.92	0.56	0.02	0.01	0.00	99.42	-2.4	0.91	
RSD (5)		0.3%	28%	2.6%	0.2%	0.2%	0.4%	0.3%	0.3%	2.7%				0.2%		0.02%	

CMI, change of mass on ignition (wt.%). Mg#, $Mg/(Mg+Fe)_{at}$.
Ref sa, reference sample; sp, spinel; gar, garnet; phl, phlogopite; lh, lherzolite; hzb, harzburgite; nd, not determined; bd, below detection.
Values for reference samples UBN and JP-1 are averages of 8 and 5 measurements respectively done on ignited powders in the same laboratory during the period when the Tariat samples were analyzed. RSD, relative standard deviation in % (1σ/mean).
[a] Data from Spettel et al. (1991).
[b] Samples analysed at Bristol laboratory.

studies (depending on availability of rock powders) as well as representative additional xenoliths. Fertile spinel lherzolites rich in clinopyroxene (cpx) are by far most common xenoliths at Shavaryn–Tsaram while refractory peridotites are very rare (Ionov, 1986), e.g. they were not reported by Press et al. (1986). In order to cover the range

of peridotite compositions of the CLM beneath Shavaryn–Tsaram more comprehensively, the rare olivine-rich, cpx-poor (≤10%) xenoliths were preferentially collected during field work. These rocks make up some 40% of samples analysed in this study, i.e. about an order of magnitude more than their estimated share among hundreds of xenoliths inspected in the outcrop. One of the Shavaryn–Tsaram xenoliths in Table 1 is garnet–spinel lherzolite; the remainder are medium to coarse-grained spinel facies rocks with modal cpx ranging from 2 to 18% and protogranular microstructures.

The majority of the xenoliths were >10 cm in size. Their outer parts were removed with a hammer or rock saw, several hundred grams of fresh material were crushed in a steel mortar, 50–100 g splits of the crushed rock were ground to powder in agate. A few of the rare cpx-poor peridotites were smaller in size, with only about 100 g of clean crushed material obtained. Some of the sampled cpx-poor rocks contain patches of silicate glass, accessory phlogopite or apatite (Press et al., 1986; Ionov et al., 1994). Macro- and microscopic observations on several very large lherzolite xenoliths (≥50 cm across, e.g. Mo-99 and 4500-26) found no cm-scale modal layering common in some peridotite massifs (Bodinier and Godard, 2003). The Shavaryn–Tsaram xenolith suite also includes subordinate pyroxenites and very rare veined peridotites (Ionov et al., 1998). Whole-rock samples were not prepared from xenoliths containing pyroxenite or basalt veins.

2.2. Analytical techniques

The majority of the samples were analysed using wavelength-dispersive X-ray fluorescence (XRF) spectrometry at the University of Mainz. The rock powders were ignited for ≥3 h at 1000° to turn all FeO into Fe_2O_3 and expel water and CO_2. Glass beads produced by fusing 0.8 g of ignited powders with 4.8 g of dried LiB_4O_7 (1:7 dilution) were analysed on a Philips PW1404 instrument using ultramafic and mafic reference rock samples as external standards. Reference samples JP-1 and UBN were analysed as unknowns to control accuracy (Table 1).

Another six Tariat xenoliths (refractory peridotites only) were analyzed using a similar technique on a Spectro XLAB 2000 EDS spectrometer at the Department of Earth Sciences, Bristol University, UK (Brooker et al., 2004). Five samples were analysed both at Bristol and Mainz laboratories. We also use here recently published whole-rock data on over 20 Vitim peridotites (except veined and composite xenoliths) obtained together with those for the Tariat suite at Mainz laboratory (Ionov et al., 2005b) as well as analyses of three more Vitim peridotites after Ionov et al. (1993). By

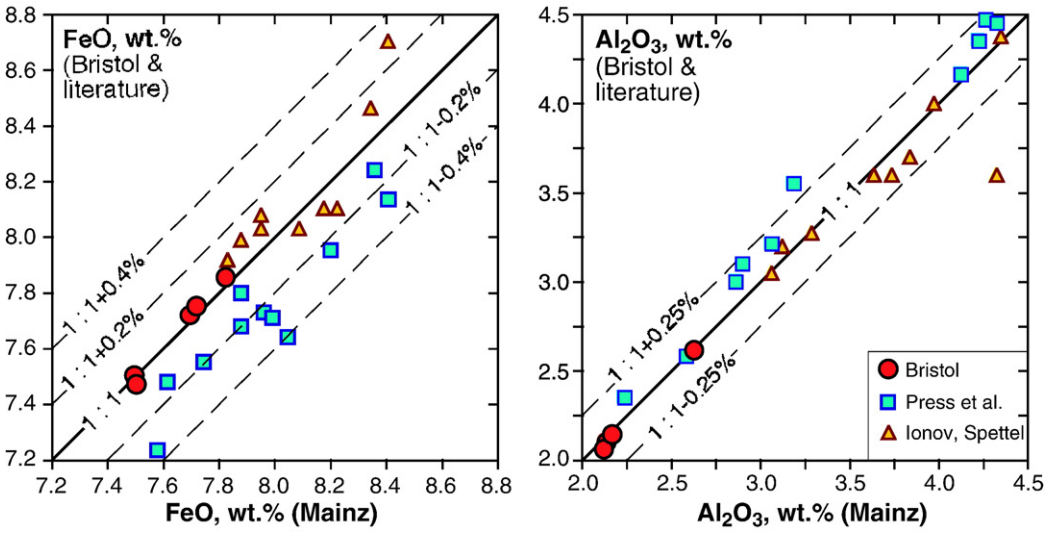

Fig. 2. Plots of FeO (a) and Al_2O_3 (b) in Shavaryn–Tsaram peridotites obtained at J. Gutenberg University (Mainz) vs. those obtained by duplicate analyses at Bristol University in this study (filled circles) and literature data (Press et al., 1986; Ionov, 1986; Spettel et al., 1991). Solid lines (1:1) show equal concentrations in the duplicated analyses, dashed lines mark differences of ±0.2% and ±0.4% in (a) and ±0.25% in (b). Note that FeO values reported by Press et al. (1986) are systematically lower while those for Al_2O_3 are higher than in this study (probably due to analytical problems); the FeO and Al_2O_3 data in (Ionov, 1986; Spettel et al., 1991) show no systematic differences but significant scatter. Data from Bristol match those from Mainz very well.

contrast to the Shavaryn–Tsaram suite, ~85% of the Vitim xenoliths are garnet and garnet–spinel peridotites (Ionov et al., 1993, 2005b). The entire dataset including published data for samples duplicated in this study is provided in Tables 1 and 2 of Electronic Supplement.

2.3. Data quality in relation to earlier work

There are good reasons to believe that it is now possible to obtain whole-rock major element composition of peridotites with better accuracy and precision than a decade or two ago. Important improvements, such as better counting statistics, have been made in new generations of energy- and wavelength-dispersive XRF spectrometers. The use of low-dilution glass beads with sample to flux ratios of 1:5 or 1:7, as used in this study, instead of 1:10, further improves data acquisition for light elements and those at low abundances. Because the XRF analyses in the Mainz and Bristol laboratories were done on ignited powders, differences in alteration degrees and iron oxidation states between the samples are not likely to affect measured element contents.

The contents of FeO and Al_2O_3 in Shavaryn–Tsaram peridotites obtained at Mainz laboratory are plotted versus those from Bristol and the literature data in Fig. 2. The five duplicates run at Mainz and Bristol reproduced to ± 0.05 wt.% for Al_2O_3 and FeO indicating that the datasets from the two laboratories are consistent. Duplicates of analyses from Ionov (1986) and Spettel et al. (1991) show no or little systematic bias but conspicuous scatter (usually within ±0.20%) relative to the 1:1 (equal concentrations) reference line. By contrast, the duplicate analyses from Mainz yield systematically higher FeO (by 0.08–0.40%) and lower Al_2O_3 (by 0.01–0.36%) values than the data from Press et al. (1986) for the same samples; because of this bias the data points plot either above (Al_2O_3) or below (FeO) the 1:1 line in Fig. 2. In addition, the data from Press et al. (1986) show much scatter on the same plots, by contrast with the duplicates from Bristol, which all plot close to the 1:1 reference line. Press et al. (1986) attributed the lower FeO in their Shavaryn–Tsaram dataset than in other mantle peridotites to "bulk chemical differences in primitive mantle the suites were derived from". Our duplicate analyses suggest that they may rather be related, at least partially, to analytical problems.

We note that the new data from Mainz closely reproduce the Fe and Al contents in peridotite reference samples JP-1 and UBN (Table 1; Ionov et al., 2005b). Moreover, duplicate analyses from this and earlier work show that the data from Mainz are consistent with high-precision analyses of peridotites from Bristol and Niigata (Ionov et al., 2005b,c; Ionov, 2007). Overall, they provide a significant improvement in data quality as well as in analysis numbers compared to the sum of previously published data on the Tariat peridotite suite.

A corollary of the comparisons between the new high-quality XRF analyses and the older literature data on Tariat xenoliths in this section is that some of the scatter of data points on Al–Fe or Mg–Fe plots for mantle peridotites in regional or worldwide compilations (Fig. 1b; McDonough, 1990; Bodinier and Godard, 2003; Palme and O'Neill, 2003) may be due to analytical uncertainties, likely reaching ±0.2–0.3% FeO. This is close to the difference in FeO contents between residues of 10% melt extraction at 1 GPa and 2 GPa (Fig. 1a), i.e. enough to "blur" evidence for melt extraction at low pressures ($P<2$ GPa) if it does exist in peridotite data sets.

Another likely reason for the "noise" in co-variation plots based on data compilations is potential sampling problems. Reliable estimates of the composition of mantle lithosphere require bulk analyses of large specimens (e.g. Boyd, 1989; Boyd et al., 1997; Ionov et al., 2005c). Mantle rocks are commonly coarse-grained and may have mm to cm-scale heterogeneities in the distribution of pyroxenes, garnet, accessory minerals and glass (e.g. Ionov et al., 1994; Ionov, 2004; Ionov et al., 2005b for Tariat and Vitim xenoliths). Analytical samples that are ideally as large as 0.5 kg are required to bridge those heterogeneities and provide representative compositional data (Boyd et al., 1997) (as is the case for the majority of fertile Tariat and Vitim peridotites in this study). Unfortunately, peridotite xenoliths of such large dimensions are rare; moreover, their outer parts are likely to contain veins of host magma and alterations products and should be avoided when sampling. As a result, analyses in the literature may be done on samples that are too small or too altered to be representative; some reported bulk compositions are calculated from mineral analyses and modal estimates (e.g. Bernstein et al., 1998). Some workers intentionally report analyses of veined and composite peridotites (Le Roux et al., 2007). Certain mantle peridotites (wehrlites, dunites) cannot be partial melting residues (e.g. Kelemen et al., 1998). Overall, the use of limited numbers of carefully selected data on representative samples, as in this study, may have obvious advantages in assessing melting relationships in the mantle compared to comprehensive, but poorly "filtered" compilations of any available chemical data on mantle peridotites.

3. Distinguishing residual and metasomatised peridotites

Metasomatic enrichments in iron can be an order of magnitude higher than the analytical uncertainties

discussed in the previous section, with FeO contents in the enriched rocks as high as 10–16% (e.g. Lee and Rudnick, 1999; Bodinier and Godard, 2003; Ionov et al., 2005a) compared to <8.5% in melting residues (Fig. 1a). Because we intend to look at the compositions of initial melting residues, it is imperative to avoid peridotite series affected by pervasive metasomatism and also to identify and discard odd individual samples with significant Fe-enrichments. The main reason why the Tariat and Vitim xenolith suites have been selected for this study is that lherzolites in those suites are little affected by metasomatism. In particular, rocks containing amphibole, phlogopite, late-stage clinopyroxene or silicate glass are rare and mainly occur among the subordinate refractory, olivine-rich peridotites (Ionov, 1986; Ionov et al., 1994); more fertile xenoliths predominant in both suites are typically low in light relative to heavy rare earth elements and have depleted Sr, Nd and Hf isotope compositions (Press et al., 1986; Stosch et al., 1986; Ionov et al., 1993, 2005b,d).

The content of Al_2O_3 is considered a robust partial melting index in residual peridotites because it rapidly decreases as partial melting proceeds at any depth (Walter, 2003; Herzberg, 2004) and is less affected by post-melting processes than other major oxides. This is illustrated by the correlation between MgO and Al_2O_3 for the central Asian peridotites, which is nearly independent of pressure (Fig. 3a). By comparison, a plot of FeO vs. Al_2O_3 has a broad scatter (7.3–9.8% FeO) for highly refractory peridotites (Al_2O_3<2%; Fig. 3b). Experimental data show that FeO ≥8.5% cannot be produced by partial melting of normal fertile mantle (~8% FeO) at any pressure (Walter, 2003; Herzberg, 2004). For this reason we attribute such high FeO to post-melting percolation of Fe-rich melts. Earlier studies have documented widespread Fe-enrichments in refractory peridotites in the nearby Siberian craton (Boyd et al., 1997; Ionov et al., 2005a) and elsewhere (Lee and Rudnick, 1999; Smith, 2000; Takazawa et al., 2000; Peslier et al., 2002; Bodinier and Godard, 2003). They appear to be a major reason for the broad FeO variations in on-craton peridotite xenoliths (6 to >9%; Fig. 1b) and may be related to better permeability of olivine-rich rocks compared to pyroxene-rich lherzolites (Bodinier et al., 1988; Toramaru and Fujii, 1986). We disregard the refractory rocks with Al_2O_3<2% in the discussion of partial melting phenomena in the next section because of difficulties in telling rare pristine olivine-rich melting residues from the common metasomatised, Fe-enriched rocks. Moreover, as shown in the next section, the key feature of our data set, i.e. a

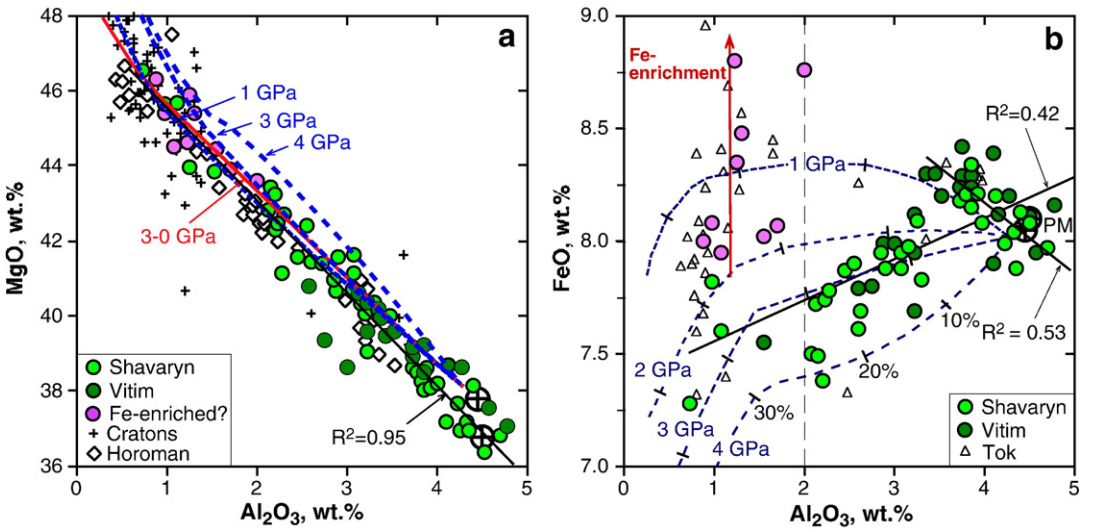

Fig. 3. Plots of Al_2O_3 vs. MgO (a) and FeO (b) in peridotite xenoliths from the Tariat (Shavaryn–Tsaram) and Vitim volcanic fields in central Asia (filled circles) in comparison with equilibrium melting residues at 1 to 4 GPa. Also shown in (b) are peridotites from Tok (SE Siberian craton, empty triangles), which are strongly affected by post-melting percolation of low-Mg-number basaltic melts (Ionov et al., 2005a). We infer, on the basis of the melting trends and comparisons with the Tok xenoliths, that significant Fe-enrichments took place in those refractory (<2% Al_2O_3) Tariat peridotites that plot above the 2 GPa melting trend (light fill). The remainder of the central Asian xenoliths (darker fill) shows a poor linear (positive) Fe–Al correlation (correlation coefficient, R^2=0.42). By contrast, both normal and Fe-enriched central Asian xenoliths define a good (negative) linear Mg–Al correlation (R^2=0.92), also overlapping the Mg–Al trends for the Horoman peridotites and least refractory (>1% Al_2O_3) cratonic xenoliths (symbols are the same as in Fig. 1).

negative Fe–Al correlation indicating melt extraction at low pressures, is mainly seen in the high–Al residues of low melting degrees; hence the highly refractory, low-Al rocks are of little relevance to the subject of this study.

The remaining 56 peridotites with >2% Al_2O_3 in our data base have FeO ≤8.4% (except a single sample with 8.8% FeO), i.e. within the FeO range in experimental melting residues. In order to screen them for odd rocks affected by melt metasomatism we use a plot (Plate 1a of Electronic Supplement) of Al vs. Ti, a minor element which commonly shows strong enrichments in metasomatised Fe-rich rocks (e.g. Menzies et al., 1987; Bodinier and Godard, 2003). The majority of the Tariat and Vitim lherzolites define a positive Al–Ti correlation controlled by melt extraction (Press et al., 1986; Wiechert et al., 1997; Takazawa et al., 2000; Ionov, 2007), but four samples with TiO_2/Al_2O_3 >0.05 plot off that trend towards higher TiO_2 (labelled on Plate 1a of Electronic Supplement). They include a single Tariat peridotite with abundant phlogopite (4230-16 Press et al., 1986) and the lherzolite with 8.8% FeO; these four samples (out of 56) are considered as metasomatised (listed in Table 2 of Electronic Supplement).

4. Discussion

4.1. Al–Fe relationships in the Tariat and Vitim peridotite xenoliths

The remaining "normal" peridotites have Al_2O_3 range 2–5% and show an overall, but poorly defined, positive Al–Fe correlation (R^2 =0.42; Fig. 3b). This correlation is not seen in Fig. 1b for a larger peridotite dataset (Canil, 2004), possibly because of the reasons discussed in Sections 1 and 2. The Fe–Al relationships in Fig. 3 seem to indicate an overall decrease in iron during melt extraction, which can be interpreted as a result of partial melting at moderate pressures (3–4 GPa). Alternatively, it can be seen as broadly consistent with the assertions of Palme and O'Neill (2003) that iron is essentially constant in off-cratonic peridotites.

However, closer inspection of the data suggests that in the most fertile peridotites (Al_2O_3 >3.4%), there is a negative correlation between Al and Fe (R^2 =0.53; Fig. 3b). This is much more clearly visible if the data are averaged in intervals of 0.25% Al_2O_3 increments (Fig. 4a) or in a sliding window with a width of 0.4% Al_2O_3 moving in 0.1% Al_2O_3 steps (Fig. 4b). The averaging procedure used in Fig. 4 (see figure captions for details) has the advantage of weighting all "depletion intervals" (e.g. measured in terms of 0.25% Al_2O_3 decrements in Fig. 4a) equally and thus showing both the enrichment and

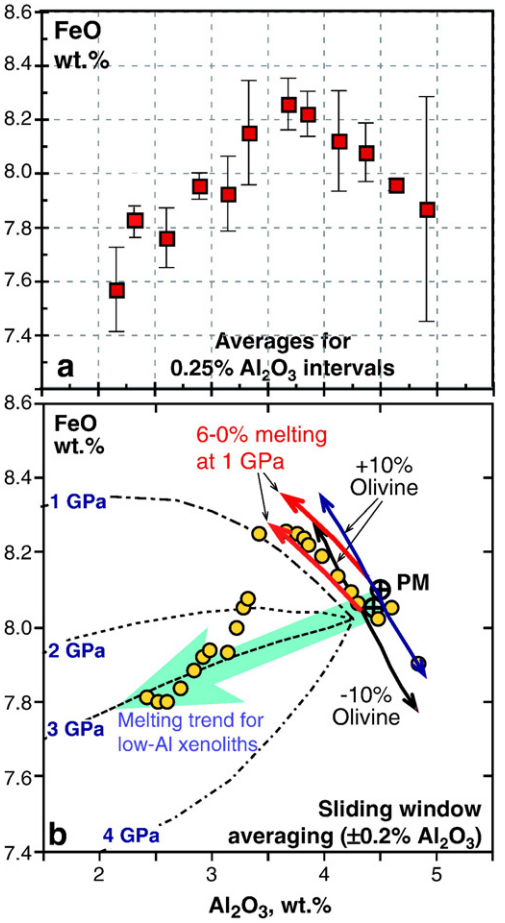

Fig. 4. Plots of Al_2O_3 vs. FeO in central Asian peridotites with 2%< Al_2O_3 <5% averaged over intervals of 0.25% Al_2O_3 (a), and using a "sliding window" method with 0.1% Al_2O_3 steps and ±0.2% Al_2O_3 averaging intervals (b). Specifically, the data points shown in (a) as squares were obtained by averaging FeO and Al_2O_3 contents for xenoliths with Al_2O_3 ranging from 2.00 to 2.24%, 2.25 to 2.49%, 2.5 to 2.74% etc. The data points shown in (b) as circles are averages of FeO and Al_2O_3 contents for xenoliths with Al_2O_3 ranging from 2.00 to 2.4%, 2.1 to 2.5%, 2.2 to 2.6% etc. Vertical bars in (a) show ±1σ for each FeO average; the magnitude of FeO variations greatly exceeds the uncertainties of individual averages. Thick transparent arrow in (b) is a melting path at ~3 GPa inferred for peridotites with 2–3.4% Al_2O_3. Lighter arrows in (b) are residues of 0–6% partial melting at 1 GPa calculated using as source compositions two Tariat peridotites with higher Al_2O_3 than that in the experimental work (Herzberg, 2004). Dark arrows are for late-stage olivine crystallisation and/or "metamorphic differentiation" models assuming either addition or removal of 0–10% of olivine from the same two Tariat peridotites. Removing olivine is equivalent to adding pyroxenes and spinel of the same composition and in the same proportions as they occur in the initial rock (relevant both to metamorphic differentiation and "refertilization"). The Al–Fe relationships of the central Asian peridotites are matched by 0–6% of shallow (1 GPa) partial melting of primitive mantle for rocks with >3.4% Al_2O_3 and higher degrees of melting at 2–4 GPa for less fertile peridotites, but are at odds with the addition of either spinel websterite (opx+cpx+spl) or olivine to less fertile or more fertile peridotites, respectively.

depletion trends of iron clearly, i.e. not overshadowed by Al–Fe scatter in individual samples.

This negative Al–Fe correlation has not been noticed in previous studies, probably because fertile peridotites with over 4% Al_2O_3 are rare (McDonough, 1990; Pearson et al., 2003) and are therefore seriously underweighted in plots of global and regional peridotite data. For example, lherzolites with $4.0\% < Al_2O_3 < 5.4\%$ make up only ~6% out of over 700 off-craton peridotite xenoliths in the compilation of (Canil, 2004); about a third of them are Vitim and Tariat peridotites from earlier studies (Press et al., 1986; Ionov et al., 1993). In addition, analytical and sampling uncertainties and random Fe-enrichments are likely to obscure the "bent" Al–Fe trend and make it look more like a random scatter of the FeO values as discussed in Section 2. This study overcomes those problems because it is based on high-quality data mainly obtained in a single laboratory. It is also possible that this type of the Al-Fe trend is not ubiquitous in the off-cratonic lithospheric mantle worldwide but may occur only in lithospheric domains with specific tectonic settings.

4.2. The Al–Fe trend in the context of partial melting

The convex-upward Fe–Al trend is not consistent either with equilibrium partial melting at any specific single depth (pressure) or polybaric decompression melting (e.g. from 3 to 0 GPa, Figs. 1a and 4b). However, the trend can be explained if one assumes that the central Asian xenoliths represent two groups of melt extraction residues that have the same fertile source but went through distinct melting histories: the Al-rich peridotites are produced by partial melting at low pressures (~1 GPa) whereas the more refractory peridotites are residues of partial melting at greater depths (2–4 GPa) and higher melt extraction rates (Figs. 3b and 4b). In such a case, the contents of FeO (~8.0%) and Al_2O_3 (~4.5%) in the inferred fertile source (common to both groups) are similar to "primitive mantle" (PM) estimates (McDonough and Sun, 1995; Palme and O'Neill, 2003). In other words, what looks like a single hump-shaped trend in Fig. 4 is interpreted here as a superposition of two distinct melting trends, both originating near the PM composition. One of them (the negative Al–Fe correlation) corresponds to low degrees (≤6%, Fig. 4b) of shallow (~1 GPa) partial melting. The other trend (a poor positive Al–Fe correlation at $Al_2O_3 < 3.4\%$) is for residues of moderate to high degrees of melt extraction at 3±1 GPa (thick transparent arrow in Fig. 4b). We speculate that samples corresponding to low melting degrees for the second trend (Al_2O_3 from 3.4 to ≥4%) are either missing or very rare in our data set. Thus, the apparent continuity of the overall averaged trend in Fig. 4a on the low-Al side of the "hump" is an artefact of the averaging procedure in the Al_2O_3 range where the "high-Al, low-P" and the "low-Al, high-P" trends overlap because the averaging interval (0.25–0.4%) includes samples belonging to distinct trends; this is seen as elevated standard errors on FeO averages (Fig. 4a). It is also likely that some samples with 3–3.5% Al_2O_3 are transitional between the low-P and high-P trends, i.e. have melting pressures from 1 to 4 GPa. The complex "dual" nature of the Al–Fe relationships in our data set is more evident in Fig. 4b where the "sliding window" averages cluster around the 3 GPa melting trend at 2.3–3.3% Al_2O_3.

Some of the fertile central Asian peridotites have somewhat higher Fe and Al contents than the 1 GPa experimental melting trend in Figs. 3b and 4b. The bias may be related to the fact that the initial peridotite in the melting experiments (Herzberg, 2004) is less fertile (e.g. has lower Al) than most likely PM estimates (McDonough and Sun, 1995; Palme and O'Neill, 2003; Ionov, 2007). To check this hypothesis we calculated residue compositions for 0–6% partial melting using as starting compositions two Tariat peridotites with Al and Fe contents close to the PM values (McDonough and Sun, 1995; Palme and O'Neill, 2003; Ionov, 2007). Extracted melt compositions were taken to be the same as in reference (Herzberg, 2004) for each melting degree. The two model melting trends bracket the compositions of the central Asian peridotites in Fig. 4b. One xenolith (Mo-105 with 5.07% Al_2O_3) is too Al-rich for a melting residue; it may contain a pyroxenite vein overlooked during sample preparation or may have been metasomatised (Press et al., 1986). We conclude that the Al–Fe relationships in the fertile peridotites (3.5–4.8% Al_2O_3) can be explained by shallow partial melting of a source with major element composition similar to primitive mantle models. The Al–Fe relationships in the total xenolith suite in this study are consistent with a partial melting origin assuming that they represent residues of melt extraction both at shallow and at moderate depths.

4.3. Alternative origins for the Al–Fe trends and fertile CLM?

We also need to consider a possibility that the complex Al–Fe relationships in our data set are caused by other processes than partial melting. Chemical variations in fertile mantle peridotites were earlier attributed to various post-melting processes, like metamorphic differentiation (Press et al., 1986; Palme and O'Neill, 2003), late-stage olivine crystallisation

(Niu et al., 1997), porous flow (Asimov, 1999), and refertilization (Elthon, 1992; Saal et al., 2001; Bodinier and Godard, 2003). Some authors (Le Roux et al., 2007) even claim that the majority of lherzolites exposed at the Earth surface (including off-craton mantle xenoliths) record refertilization processes.

From such a viewpoint, the most likely conjecture based on the shape of the Al–Fe trend in Figs. 3b and 4 could be that chemical variations for highly to moderately refractory rocks (1 to 3.5% Al_2O_3) result from melt extraction whereas those at >3.5% Al_2O_3 are due to a post-melting process. There may be several ways to assess the viability of such hypotheses.

(a) The first one is of a general nature and could be applied to any of the alternatives. In the model of melt extraction from a primitive source advocated here, the only component expected to be sensitive to melting conditions, like pressure, is iron. Co-variation plots of other major elements should be reasonably smooth and continuous in the whole melting range (~1–4.5% Al_2O_3 in the residues) for P=1–4 GPa (Walter, 2003; Herzberg, 2004). The contrary should be the case for any alternative two-stage model (melting for ~1–3.5% Al_2O_3, another process for >3.5% Al_2O_3) because it is highly unlikely that both melt extraction and any other processes should yield identical chemical trends. Thus, for two-stage models, the "bend" in the Al–Fe trend at ~3.5 Al_2O_3 has to be mirrored by equivalent bends or unusual scatter on co-variation plots of other major and minor elements.
The latter is not the case for the Mg–Al plot (Fig. 3a), where the central Asian peridotites show a regular linear trend (R^2=0.95) matching melting experiments at 1–4 GPa. Plots of other oxides vs. Al_2O_3 are shown in Fig. 5 and Plate 1 of Electronic Supplement. Most of them define regular linear trends as well (e.g. R^2=0.94 for Ca and Ni), and none has a bend at ~3.5 Al_2O_3. Cr is not correlated with Al (R^2=0.0) and its contents are very constant at >2.5% Al_2O_3 (Fig. 5b); Cr scatter at <2.5% Al_2O_3 may be due to smaller sample size of some refractory peridotites in our data set and heterogeneous distribution of Cr-rich spinel ("nugget effect" after Canil (2004). Also shown on many of these plots are data from the Mainz laboratory on spinel lherzolites from Zala, another volcano from the Tariat region, obtained in a different project (Ionov, 2007). The Zala xenoliths closely follow all the trends (including Al–Fe) shown by the Shavaryn–Tsaram and Vitim suites.
Ca/Al increases from ~1.05 at 4–5% Al_2O_3 to ~1.25 at 2% Al_2O_3 (Fig. 5c) without a bend in the middle, which is particularly evident if Ca/Al values are averaged for 0.25% Al_2O_3 increments (Fig. 5d) in the same manner as for FeO (Fig. 4a). Our data confirm that Ca/Al in shallow melting residues increases with melt extraction rates and thus address a seeming controversy regarding Ca/Al in global peridotite data compilations, which typically yield higher average Ca/Al (≥1.2) than the chondritic value of 1.1 (e.g. McDonough, 1990; Palme and O'Neill, 2003). This is because moderately refractory peridotites, which tend to have high Ca/Al (Fig. 5c, d), are predominant in off-craton CLM worldwide. By contrast, the most fertile central Asian xenoliths have near-chondritic Ca/Al. Thus, chemical co-variation trends for the Tariat and Vitim peridotites at ~1–4.5% Al_2O_3 can be fully explained by partial melting of a PM-like source alone and do not call for alternative processes regarding the origin of the fertile lherzolites.

(b) Mg-numbers of olivine from the central Asian spinel lherzolites are positively correlated with Cr/(Cr+Al) in spinel and negatively correlated with whole-rock Al_2O_3 contents (Fig. 6a, b). These correlations are consistent with extraction of partial melts from a very fertile source (Mg-number ~0.89, Al_2O_3 ≥4.5%) (Press et al., 1986; Ionov, 2007), but rule out models relating whole-rock chemical variations in the fertile central Asian xenoliths to additions of variable amounts of pyroxenes and spinel to a refractory peridotite source through crystallisation from a basaltic melt impregnating the source ("refertilization" after Le Roux et al., 2007).

(c) Metamorphic differentiation (Press et al., 1986; Palme and O'Neill, 2003; Ionov, 2004) implies recrystallisation of an initially homogeneous melting residue to yield complementary zones or layers enriched either in olivine or in pyroxenes and spinel. This process, together with late-stage olivine crystallisation (Niu et al., 1997), is simulated here by adding or removing 1–10% of olivine (using measured olivine compositions) to/from the same two near-primitive Tariat peridotites. Removing olivine is equivalent to adding spinel websterite to the initial rock (i.e. by "refertilization", see previous paragraph). These models (dark arrows in Fig. 4b) show poor matches with the natural Fe–Al trend. Heterogeneous nucleation and growth of garnet during

spinel–garnet facies transition invoked earlier to explain minor scatter of some Vitim xenoliths relative to the Mg–Al trend (Fig. 3a) (Ionov, 2004) cannot produce the negative Fe–Al correlation in Fig. 4b. The latter persists even if the Vitim suite is omitted.

(d) Mantle metasomatism can precipitate clinopyroxene and thus enrich peridotites in Ca, but not so much in Al. The Ca/Al ratio is very sensitive to metasomatic cpx enrichments (e.g. Ca/Al is high in wehrlites Ionov et al., 2005a; Yaxley et al., 1991). The fact that Ca/Al in the central Asian lherzolites is *negatively* correlated with Al_2O_3 (Fig. 5c) rules out the cpx precipitation as a means to produce fertile, Al-rich lherzolites from refractory protoliths. Moreover, the precipitation of cpx is often accompanied by enrichments in Fe and phosphates (Yaxley et al., 1991; Smith, 2000; Peslier et al., 2002; Ionov et al.,

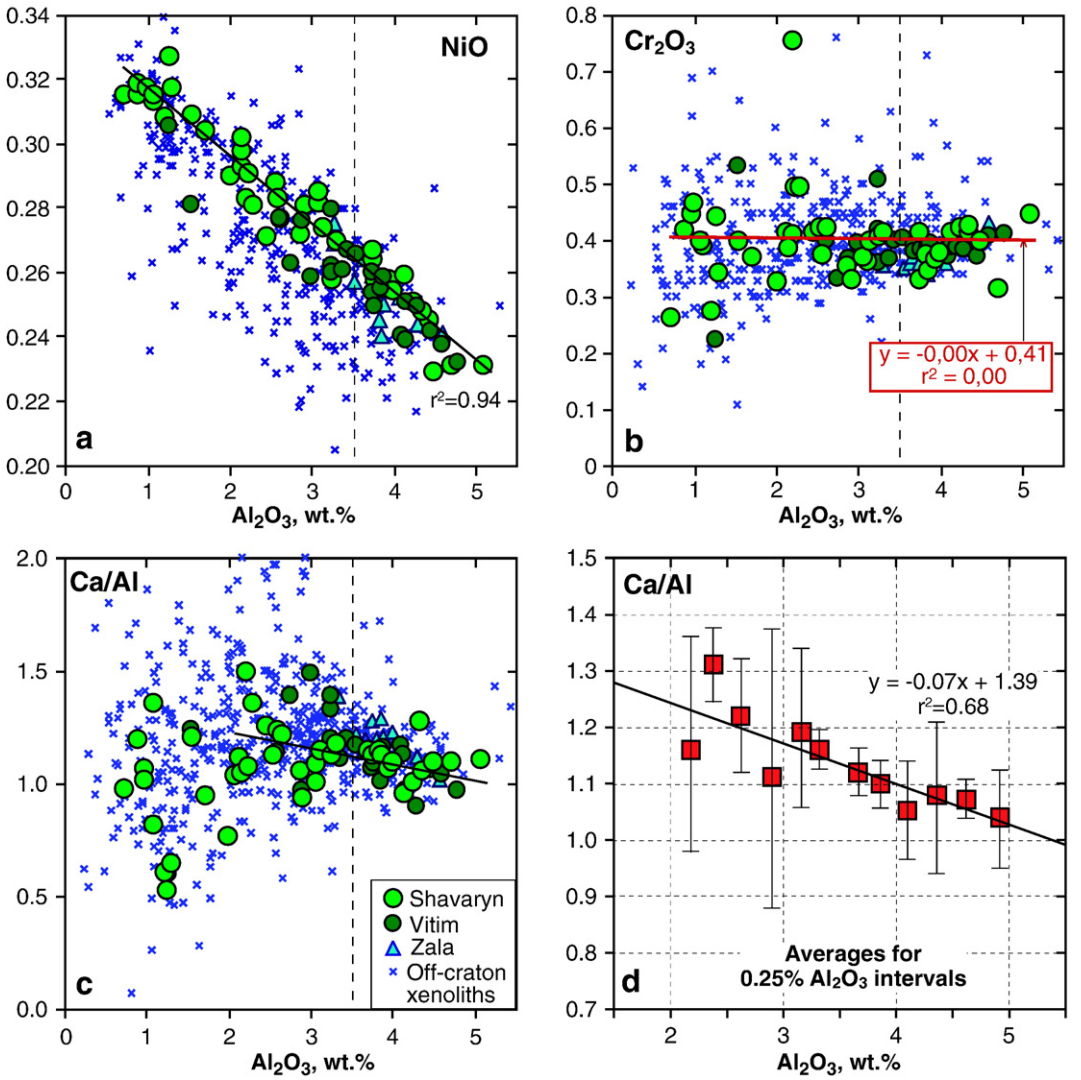

Fig. 5. Plots of Al_2O_3 vs. NiO (a), Cr_2O_3 (wt.%) (b) and Ca/Al (c) in Shavaryn–Tsaram (larger filled circles) and Vitim (smaller circles) xenoliths, with linear regression lines for the Shavaryn–Tsaram suite in (a, b) and for all the central Asian peridotites in (c). Also shown are off-craton peridotite xenoliths from worldwide localities (diagonal crosses) after (Canil, 2004) and from Zala in Tariat (Ionov, 2007) (filled triangles). Note the strong negative Al–Ni correlation ($r^2=0.94$), the absence of Al–Cr correlation ($r^2=0.0$) and a weak Al–Ca/Al correlation. Vertical dashed lines mark the position of the "hump" on Al–Fe plots (Figs. 3b and 4). (d) Ca/Al and Al_2O_3 in the Shavaryn–Tsaram and Vitim peridotites averaged in the same manner (for $2\% < Al_2O_3 < 5\%$ over intervals of 0.25% Al_2O_3) as in Fig. 4a. Note a consistent increase in averaged Ca/Al as Al_2O_3 decreases from 5 to 2% (and no "hump" at 3.5% Al_2O_3).

2005a); these are common in the refractory (Ionov et al., 1994, 2006), but not in the fertile, xenoliths in our dataset.

(e) The term "refertilization" has been increasingly used lately instead of modal or cryptic metasomatism (Frey and Green, 1974; Dawson, 1984) to describe any late-stage additions of "basaltic components" to massif peridotites and CLM xenoliths by melt infiltration (e.g. Le Roux et al., 2007; Bianchini et al., 2007). The change in terminology may be purely semantic in many cases but it might also make the impression that creating fertile lherzolites which are chemically identical to pristine, PM-like mantle, like those in this study, must be a natural end-result of mantle enrichment processes. The latter however is rather unlikely because it requires adding back the major and trace "basaltic components" to hypothetical refractory protoliths in the same proportions and quantities as they were extracted during partial melting.

Le Roux et al. (2007) recently argued that lherzolites in the Lherz massif do not represent "pristine mantle" or melt extraction residues but are secondary rocks formed by refertilization of harzburgites. Assessing the origin of massif peridotites is beyond the subject and the means of this paper. We disagree, however, with the claim in the paper by Le Roux et al. (2007) that fertile off-craton lithosphere may be viewed as the ultimate transformation of cratonic lithosphere after one or several cycles of igneous refertilization. We note that Le Roux et al. (2007) do not indicate what they consider as shortcomings of the widely accepted partial melting concept (Walter, 2003; Palme and O'Neill, 2003 and references therein) that have to be addressed by their alternative model and they do not show why and how exactly the refertilization could reproduce the sum of chemical variation trends typical of the fertile CLM (McDonough, 1990; Pearson et al., 2003; Canil, 2004, this study). An important specific point in their paper (Le Roux et al., 2007) concerns trends outlined on Cr–Al plots for samples from the Lherz massif that include peridotites, pyroxenites, but also composite samples consisting of various proportions of pyroxenite veins in peridotites. Such Cr–Al trends are not seen on plots for off-craton mantle peridotites from this study (Fig. 5b) or previous work (Canil, 2004). Overall, in spite of the growing number of studies that document local enrichments of refractory CLM in basaltic components by melt metasomatism or refertilization (Le Roux et al., 2007 and references therein), we see no need to rule out melt extraction as the principal process responsible for the formation of the fertile off-craton mantle.

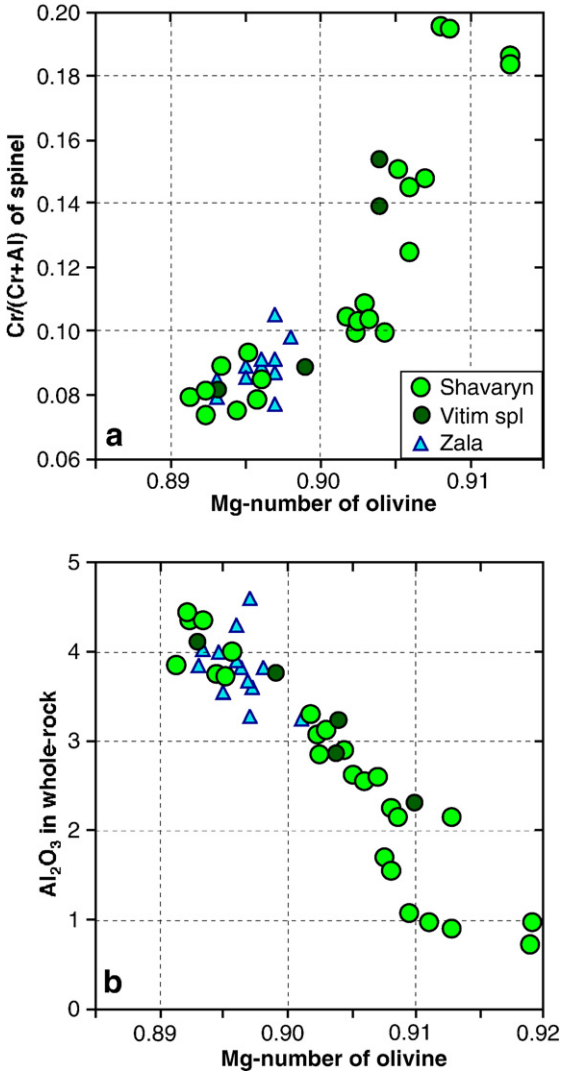

Fig. 6. Plots of olivine Mg-numbers [$Mg/(Mg+Fe)_{at}$] vs. $Cr/(Cr+Al)_{at}$ in spinel (a) and whole-rock Al_2O_3 (b) in central Asian xenoliths. Mineral data available for about half the Shavaryn–Tsaram xenoliths in this study are from Table 2 of Electronic Supplement; those for spinel peridotites from Zala and Vitim are from Ionov et al. (2005b) and Ionov (2007). A positive correlation in (a) and a negative correlation in (b) are consistent with extraction of partial melts from a very fertile source (Mg-number $\sim$0.89, $Al_2O_3 \geq 4.5\%$). These correlations also rule out any models relating whole-rock chemical variations in the fertile central Asian xenoliths to additions of variable amounts of pyroxenes and spinel to a refractory peridotite source, i.e. through crystallisation from a basaltic melt impregnating a harzburgite (Le Roux et al., 2007). Symbols are the same as in Fig. 5.

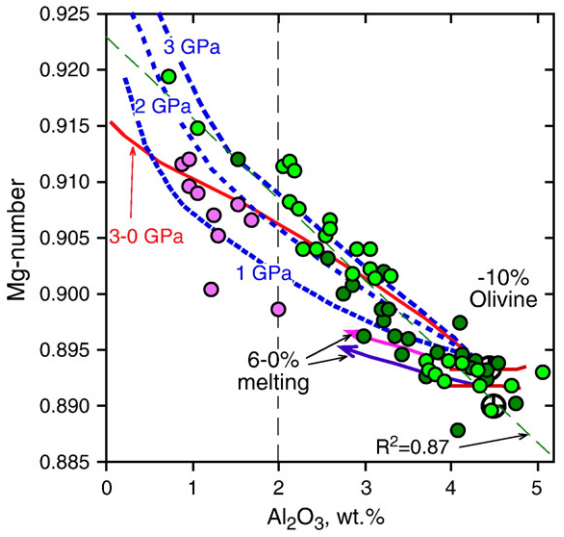

Fig. 7. A plot of Al_2O_3 vs. Mg-numbers in central Asian peridotites. Note that Mg-numbers show little variation for Al_2O_3 3.5–5%, i.e. low partial melting degrees because of high FeO in residues of shallow partial melting. Symbols are the same as in Fig. 3.

4.4. The provenance of off-craton CLM peridotites

If the conclusions on partial melting conditions responsible for the origin of the central Asian peridotite xenoliths in this study are correct they have several important petrologic and geodynamic implications.

Mg-number in mantle peridotites (or their olivines) is commonly used as an indicator of partial melting degrees and is thought to be roughly proportional to melting degrees they experienced. In particular, Mg-number in melting residues is assumed to be positively correlated with modal olivine and negatively correlated with Al and Ca (Boyd, 1989; Walter, 2003; Pearson et al., 2003). Such correlations are also seen in the xenoliths from this study (Figs. 6 and 7). However, the central Asian peridotites show a relatively narrow Mg-number range and a less pronounced Al–Mg-number trend at 3.5–5% Al_2O_3 (i.e. for shallow melting residues) than in more refractory (and unmetasomatised) xenoliths (Fig. 7). The latter feature may be typical of the shallow partial melting in regions of thinned lithosphere, like continental rifts. Thus, Mg-number appears to be a less universal indicator of partial melting degrees than commonly assumed, both because of the effects of melting depth and because of common late-stage Fe-enrichments in refractory peridotites (Kelemen et al., 1992; Bodinier and Godard, 2003). Cr/(Cr+Al) in spinel, may be a more reliable partial melting indicator (Hellebrand et al., 2001; Ionov et al., 2005c; Ionov, 2007), although one should note that the latter may also depend on temperature because of temperature-controlled Al-Cr exchange with coexisting pyroxenes (Sachtleben and Seck, 1981; Witt-Eickschen and Seck, 1991). In general, the effects of variable melting depth on Mg-numbers and of Cr–Al redistribution between spinel and pyroxenes in the residues on cooling may account for the complexity of the relationships (and common lack of clear-cut trends) between Mg-number of olivine and Cr/(Cr+Al) of spinel in mantle peridotites (e.g. Ionov et al., 2005c).

The origin of lithospheric mantle domains with the Al–Fe relationships shown in Figs. 3 and 4 is not immediately clear. One can envisage a scenario (Fig. 8), in which a body of rising fertile mantle has higher temperature in the middle than at the margins, and thus the partial melting in its centre begins at higher pressures (greater depth) and produces more refractory residues. By contrast, the colder envelope of the rising body starts to melt at low pressures (<2 GPa) and hence only experiences low degrees of partial melting. This yields high-Al peridotites, which closely follow the low-P (~1 GPa), low melting-degree (0–6%) melt extraction trend (Figs. 3b and 4b). In this case, the CLM in central Asia is a composite of melting residues initially produced in a broad range of pressures (4–1 GPa;

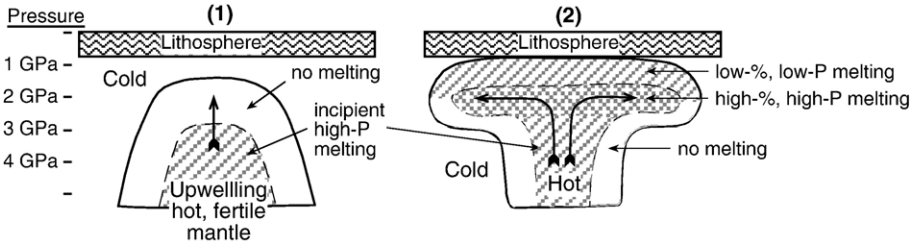

Fig. 8. A cartoon illustrating the possible (or "suggested") relationship between the depth and degrees of partial melting in a mantle diapir. (a) The upwelling material has a hot core and colder margins (the latter lose heat by conduction and mixing with surrounding mantle). Partial melting starts in the hot central portion of the diapir at greater depths (e.g. 3–4 GPa) than in the margins (~1 GPa). When the cold, viscous roof of the diapir reaches the bottom of the lithosphere it stalls and prevents the deeper hot material from rising further. Thus, the hotter material melts at 4–2 GPa (and to high degrees) while the colder material undergoes only low degrees of shallow melting.

Fig. 3b). Subsequently, the rocks were emplaced and re-equilibrated at levels corresponding to 1.2–2.3 GPa (Ionov et al., 1998, 2005b; Ionov, 2007). A likely geodynamic environment for such a melting process is a mantle upwelling in a continental region with thin lithosphere or in an oceanic domain (Takazawa et al., 2000). One such scenario could be the accretion of oceanic plateaux followed by crustal and lithospheric thickening (Niu et al., 2003; Herzberg, 2004).

Specifying a tectonic setting and a mechanism for the origin of the central Asian peridotite suites, however, is beyond both the objectives and the means of this study. Here, we wish primarily to draw attention to the fact that major element composition of a specific suite of peridotites, but possibly residual peridotites in other off-craton CLM domains, indicates a derivation in a much broader depth range (~30–130 km) than their current depth of origin (40–70 km). In particular, the iron contents in many fertile rocks are consistent with partial melting at shallow depths (≤30–40 km, ~1 GPa) and hence indicate an origin in domains with a thinner lithosphere than typical of modern off-craton intra-continental regions.

Thus, an important implication of our results is that the depth of equilibration of mantle peridotites estimated by thermo-barometry is not necessarily a good guide for constraining the original depth of formation of such rocks. We may distinguish three stages during formation of lithospheric mantle. Extraction of melts initially controls the bulk composition of these rocks (as shown in this paper). Subsequently, tectonic processes may emplace them at different depths. Finally, metamorphic equilibration redistributes chemical elements between the constituent minerals. Conventional thermo-barometry only measures this final process.

5. Conclusions

(1) We report the finding of a negative Fe–Al correlation in a series of relatively fertile off-craton mantle peridotites, which preserve an undisturbed record of partial melting in their major element compositions. This finding furnishes first natural evidence for the experimentally predicted increase in iron contents at low degrees of shallow (~1 GPa) partial melting of fertile mantle. Thus, it provides a fundamental missing link in the global petrologic models that relate the formation of the lithospheric mantle to melt extraction processes. It also sheds new light on the origin of chemical heterogeneities (and hence distinct physical and dynamic properties) of the upper mantle.

(2) We show that melt extraction ultimately responsible for the formation of the off-craton lithosphere took place at depths between 30 to 130 km. Previously used depth indicators given by classical thermo-barometry often yield very different depths. We explain this by the deformation and thickening processes during plate collisions and “orogeny”, which affect not only the crust itself but also the underlying lithosphere, i.e. the rigid substrate of the continental crust. If this scheme is correct, it may follow that the off-craton mantle may be much more robust and resistant to later tectono-magmatic events, than previously thought.

(3) We show that alternative mechanisms for the origin of fertile mantle peridotites, like late-stage refertilization of depleted refractory mantle by evolved magmas or metamorphic differentiation, fail to explain the co-variations of whole-rock and mineral compositions in the xenoliths from this study and cannot provide viable alternatives to the concept of the formation of the off-craton CLM by melt extraction from pristine mantle. In general, the findings of this study reinforce the partial melting models versus alternative explanations for the major element variations in the mantle.

Acknowledgements

DAI thanks A. Goreglyad and V. Kovalenko of Russian Academy of Sciences who participated in the fieldwork; N. Groschopf, A. Friedrichsen and R. Brooker assisted with XRF analyses. XRF analyses at Bristol University in 2002 were done using funding and facilities of the European Geochemical Facility. Reviews by J.-L. Bodinier and E. Hellebrand and editorial handling by R. Carlson helped to improve the original version of the paper.

Appendix A. Supplementary data

Supplementary data associated with this article can be found, in the online version, at doi:10.1016/j.epsl.2007.07.036.

References

Asimov, P.D., 1999. A model that reconciles major- and trace-element data from abyssal peridotites. Earth Planet. Sci. Lett. 169, 303–319.

Bernstein, S., Kelemen, P.B., Brooks, C.K., 1998. Depleted spinel harzburgite xenoliths in Tertiary dykes from East Greenland: restites from high degree melting. Earth Planet. Sci. Lett. 154, 219–233.

Bianchini, G., Beccaluva, L., Bonadiman, C., Nowell, G., Pearson, G., Siena, F., Wilson, M., 2007. Evidence of diverse depletion and metasomatic events in harzburgite–lherzolite mantle xenoliths

from the Iberian plate (Olot, NE Spain): implications for lithosphere accretionary processes. Lithos 94, 25–45.
Bodinier, J.L., Godard, M., 2003. Orogenic, ophiolitic and abyssal peridotites. In: Carlson, R.W. (Ed.), Treatise on Geochemistry. The Mantle and Core, vol. 2. Elsevier, Amsterdam, pp. 103–170.
Bodinier, J.L., Dupuy, C., Dostal, J., 1988. Geochemistry and petrogenesis of Eastern Pyrenean peridotites. Geochim. Cosmochim. Acta 52, 2893–2907.
Boyd, F.R., 1989. Compositional distinction between oceanic and cratonic lithosphere. Earth Planet. Sci. Lett. 96, 15–26.
Boyd, F.R., Pokhilenko, N.P., Pearson, D.G., Mertzman, S.A., Sobolev, N.V., Finger, L.W., 1997. Composition of the Siberian cratonic mantle: evidence from Udachnaya peridotite xenoliths. Contrib. Mineral. Petrol. 128, 228–246.
Brooker, R.A., James, R.H., Blundy, J.D., 2004. Trace elements and Li isotope systematics in Zabargad peridotites: evidence of ancient subduction processes in the Red Sea mantle. Chem. Geol. 212, 179–204.
Canil, D., 2004. Mildly incompatible elements in peridotites and the origins of mantle lithosphere. Lithos 77, 375–393.
Dawson, J.B., 1984. Contrasting types of upper-mantle metasomatism? In: Kornprobst, J. (Ed.), Kimberlites II. The Mantle and Crust–Mantle Relationships. Elsevier, Amsterdam, pp. 289–294.
Elthon, D., 1992. Chemical trends in abyssal peridotites: refertilization of depleted suboceanic mantle. J. Geophys. Res. 97, 9015–9025.
Frey, F.A., Green, D.H., 1974. The mineralogy, geochemistry and origin of lherzolite inclusions in Victorian basanites. Geochim. Cosmochim. Acta 38, 1023–1059.
Hanson, G.N., Langmuir, C.H., 1978. Modelling of major elements in mantle–melt systems using trace element approaches. Geochim. Cosmochim. Acta 42, 725–742.
Hellebrand, E., Snow, J.E., Dick, H.J.B., Hofmann, A.W., 2001. Coupled major and trace elements as indicators of the extent of melting in mid-ocean-ridge peridotites. Nature 410, 677–681.
Herzberg, C., 2004. Geodynamic information in peridotite petrology. J. Petrol. 45, 2507–2530.
Ionov, D.A., 1986. Spinel peridotite xenoliths from the Shavaryn–Tsaram volcano, northern Mongolia: petrography, major element chemistry and mineralogy. Geol. Carpath. 37, 681–692.
Ionov, D.A., 2004. Chemical variations in peridotite xenoliths from Vitim, Siberia: inferences for REE and Hf behaviour in the garnet facies upper mantle. J. Petrol. 45, 343–367.
Ionov, D.A., 2007. Compositional variations and heterogeneity in fertile lithospheric mantle: peridotite xenoliths in basalts from Tariat, Mongolia. Contrib. Mineral. Petrol. 154 (doi:10.1007/s00410-007-0203-y).
Ionov, D.A., Ashchepkov, I.V., Stosch, H.G., Witt-Eickschen, G., Seck, H.A., 1993. Garnet peridotite xenoliths from the Vitim volcanic field, Baikal region: the nature of the garnet–spinel peridotite transition zone in the continental mantle. J. Petrol. 34, 1141–1175.
Ionov, D.A., Hofmann, A.W., Shimizu, N., 1994. Metasomatism-induced melting in mantle xenoliths from Mongolia. J. Petrol. 35, 753–785.
Ionov, D.A., O'Reilly, S.Y., Griffin, W.L., 1998. A geotherm and lithospheric cross-section for central Mongolia. In: Flower, M.J.F., Chung, S.-L., Lo, C.-H., Lee, T.Y. (Eds.), Mantle Dynamics and Plate Interactions in East Asia, Geodynamics Series 27. Amer. Geophys. Union, Washington, DC, pp. 127–153.
Ionov, D.A., Chanefo, I., Bodinier, J.L., 2005a. Origin of Fe-rich lherzolites and wehrlites from Tok, SE Siberia by reactive melt percolation in refractory mantle peridotites. Contrib. Mineral. Petrol. 150, 335–353.
Ionov, D.A., Ashchepkov, I., Jagoutz, E., 2005b. The provenance of fertile off-craton lithospheric mantle: Sr–Nd isotope and chemical composition of garnet and spinel peridotite xenoliths from Vitim, Siberia. Chem. Geol. 217, 41–75.
Ionov, D.A., Prikhodko, V.S., Bodinier, J.L., Sobolev, A.V., Weis, D., 2005c. Lithospheric mantle beneath the south-eastern Siberian craton: petrology of peridotite xenoliths in basalts from the Tokinsky Stanovik. Contrib. Mineral. Petrol. 149, 647–665.
Ionov, D.A., Blichert-Toft, J., Weis, D., 2005d. Hf isotope compositions and HREE variations in off-craton garnet and spinel peridotite xenoliths from central Asia. Geochim. Cosmochim. Acta 69, 2399–2418.
Ionov, D.A., Hofmann, A.W., Merlet, C., Gurenko, A.A., Hellebrand, E., Montagnac, G., Gillet, P., Prikhodko, V.S., 2006. Discovery of whitlockite in mantle xenoliths: inferences for water- and halogen-poor fluids and trace element residence in the terrestrial upper mantle. Earth Planet. Sci. Lett. 244, 201–217.
Jordan, T.H., 1979. Mineralogies, densities and seismic velocities of garnet lherzolites and their geophysical implications. In: Boyd, F.R., Meyer, H.O.A. (Eds.), The Mantle Sample: Inclusions in Kimberlites and Other Volcanics, vol. 2. Am. Geophys. Union, Washington, D.C., pp. 1–14.
Kelemen, P.B., Dick, H.J., Quick, J.E., 1992. Formation of harzburgite by pervasive melt/rock reaction in the upper mantle. Nature 358, 635–641.
Kelemen, P.B., Hart, S.R., Bernstein, S., 1998. Silica enrichment in the continental upper mantle via melt/rock reaction. Earth Planet. Sci. Lett. 164, 387–406.
Kopylova, M.G., Russell, J.K., 2000. Chemical stratification of cratonic lithosphere: constraints from the Northern Slave craton, Canada. Earth Planet. Sci. Lett. 181, 71–87.
Le Roux, V., Bodinier, J.L., Tommasi, A., Alard, O., Dautria, J.M., Vauchez, A., Riches, A.J.V., 2007. The Lherz spinel lherzolite: refertilized rather than pristine mantle. Earth Planet. Sci. Lett. 259, 599–612.
Lee, C.-T., Rudnick, R.L., 1999. Compositionally stratified cratonic lithosphere: petrology and geochemistry of peridotite xenoliths the Labait volcano, Tanzania. In: Gurney, J.J., Gurney, J.L., Pascoe, M.D., Richardson, S.H. (Eds.), Proc. 7th Internatl. Kimberlite Conf. Vol I. RedRoof Design, Cape Town, pp. 503–521.
McDonough, W.F., 1990. Constraints on the composition of the continental lithospheric mantle. Earth Planet. Sci. Lett. 101, 1–18.
McDonough, W.F., Sun, S.-S., 1995. The composition of the Earth. Chem. Geol. 120, 223–253.
Menzies, M.A. (Ed.), 1990. Continental Mantle. Clarendon Press, Oxford.
Menzies, M.A., Roggers, N., Tindle, A., Hawkesworth, C.J., 1987. Metasomatic and enrichment processes in lithospheric peridotites, an effect of asthenosphere–lithosphere interaction. In: Menzies, M.A., Hawkesworth, C.J. (Eds.), Mantle Metasomatism. Academic Press, London, pp. 313–361.
Nickel, K.G., Green, D.H., 1984. The nature of the upper-most mantle beneath Victoria, Australia as deduced from ultramafic xenoliths. In: Kornprobst, J. (Ed.), Kimberlites II. The Mantle and Crust–Mantle Relationships. Elsevier, Amsterdam, pp. 161–178.
Niu, Y., Langmuir, C.H., Kinzler, R.J., 1997. The origin of abyssal peridotites: a new perspective. Earth Planet. Sci. Lett. 152, 251–265.
Niu, Y., O'Hara, M.J., Pearce, J.A., 2003. Initiation of subduction zones as a consequence of lateral compositional buoyancy contrast within the lithosphere: a petrological perspective. J. Petrol. 44, 851–866.
Palme, H., O'Neill, H.S.C., 2003. Cosmochemical estimates of mantle composition. In: Carlson, R.W. (Ed.), Treatise on Geochemistry. The Mantle and Core, vol. 2. Elsevier, pp. 1–38.
Pearson, D.G., Canil, D., Shirey, S.B., 2003. Mantle samples included in volcanic rocks: xenoliths and diamonds. In: Carlson, R.W. (Ed.),

Treatise on Geochemistry. The Mantle and Core, vol. 2. Elsevier, pp. 171–276.

Peslier, A.H., Francis, D., Ludden, J., 2002. The lithospheric mantle beneath continental margins: melting and melt-rock reaction in Canadian Cordillera xenoliths. J. Petrol. 43, 2013–2047.

Press, S., Witt, G., Seck, H.A., Eonov, D., Kovalenko, V.I., 1986. Spinel peridotite xenoliths from the Tariat Depression, Mongolia. I: Major element chemistry and mineralogy of a primitive mantle xenolith suite. Geochim. Cosmochim. Acta 50, 2587–2599.

Saal, A.E., Takazawa, E., Frey, F.A., Shimizu, N., Hart, S.R., 2001. Re–Os isotopes in the Horoman Peridotite: evidence for refertilization? J. Petrol. 42, 25–37.

Sachtleben, T., Seck, H.A., 1981. Chemical control of Al-solubility in orthopyroxene and its implications on pyroxene geothermometry. Contrib. Mineral. Petrol. 78, 157–165.

Smith, D., 2000. Insights into the evolution of the uppermost continental mantle from xenolith localities on and near the Colorado Plateau and regional comparisons. J. Geophys. Res. 105, 16769–16781.

Spettel, B., Palme, H., Ionov, D.A., Kogarko, L.N., 1991. Variations in the iridium content of the upper mantle of the Earth. Lunar Planet. Sci. Conf. XXII, 1301–1302.

Stosch, H.G., Lugmair, G.W., Kovalenko, V.I., 1986. Spinel peridotite xenoliths from the Tariat Depression, Mongolia. II: geochemistry and Nd and Sr isotopic composition and their implications for the evolution of the subcontinental lithosphere. Geochim. Cosmochim. Acta 50, 2601–2614.

Takazawa, E., Frey, F.A., Shimizu, N., Obata, M., 2000. Whole rock compositional variations in an upper mantle peridotite (Horoman, Hokkaido, Japan): are they consistent with a partial melting process. Geochim. Cosmochim. Acta 64, 695–716.

Toramaru, A., Fujii, N., 1986. Connectivity of melt phase in a partially molten peridotite. J. Geophys. Res. 91, 9239–9252.

Walter, M.J., 2003. Melt extraction and compositional variability in mantle lithosphere. In: Carlson, R.W. (Ed.), Treatise on Geochemistry. The Mantle and Core, vol. 2. Elsevier, Amsterdam, pp. 363–394.

Wiechert, U., Ionov, D.A., Wedepohl, K.H., 1997. Spinel peridotite xenoliths from the Atsagin-Dush volcano, Dariganga lava plateau, Mongolia: a record of partial melting and cryptic metasomatism in the upper mantle. Contrib. Mineral. Petrol. 126, 345–364.

Witt-Eickschen, G., Seck, H.A., 1991. Solubility of Ca and Al in orthopyroxene from spinel peridotite: an improved version of an empirical geothermometer. Contrib. Mineral. Petrol. 106, 431–439.

Yaxley, G.M., Crawford, A.J., Green, D.H., 1991. Evidence for carbonatite metasomatism in spinel peridotite xenoliths from western Victoria, Australia. Earth Planet. Sci. Lett. 107, 305–317.